Comparative analysis of ESCRT-I, ESCRT-II and ESCRT-III function in *Drosophila* by efficient isolation of ESCRT mutants

Thomas Vaccari[1,*,‡], Tor Erik Rusten[2], Laurent Menut[1], Ioannis P. Nezis[2], Andreas Brech[2], Harald Stenmark[2] and David Bilder[1,‡]

[1]Department of Molecular and Cell Biology, University of California, Berkeley, CA 94702, USA
[2]Centre for Cancer Biomedicine and Department of Biochemistry, the Norwegian Radium Hospital, University of Oslo, Montebello, N-0310 Oslo, Norway

*Current address: IFOM, Istituto FIRC di Oncologia Molecolare, Milan, Italy
‡Authors for correspondence (e-mails: thomas.vaccari@ifom-ieo-campus.it; bilder@berkeley.edu)

Accepted 16 April 2009
Journal of Cell Science 122, 2413-2423 Published by The Company of Biologists 2009
doi:10.1242/jcs.046391

Summary

ESCRT proteins were initially isolated in yeast as a single functional set of conserved components controlling endosomal cargo sorting and multivesicular body (MVB) biogenesis. Recent work has suggested that metazoan ESCRT proteins might have more functionally diverse roles, but the limited availability of ESCRT mutants in species other than yeast has hampered a thorough analysis. Here, we used a genetic screening strategy based on both cell-autonomous and non-autonomous growth-promotion phenotypes to isolate null mutations in nearly half of the ESCRT-encoding genes of *Drosophila*, including components of ESCRT-I, ESCRT-II and ESCRT-III complexes. All ESCRT components are required for trafficking of ubiquitylated proteins and are required to prevent excess Notch and EGFR signaling. However, cells lacking certain ESCRT-III components accumulate fewer ubiquitylated molecules in endosomes and display reduced degrees of cell proliferation compared with those lacking components of ESCRT-I and ESCRT-II. Moreover, although we find by ultrastructural analysis that MVB formation is impaired in ESCRT-I and ESCRT-II mutant cells, MVB biogenesis still occurs to some degree in ESCRT-III mutant cells. This work highlights the multiple cell biological and developmental roles of ESCRT proteins in *Drosophila*, suggests that the metazoan ESCRT-I, ESCRT-II and ESCRT-III complexes do not serve identical functions, and provides the basis for an extensive analysis of metazoan ESCRT function.

Supplementary material available online at
http://jcs.biologists.org/cgi/content/full/122/14/2413/DC1

Key words: ESCRT, MVB sorting, Endocytosis, *Drosophila*, Tumor suppression genes

Introduction

The sorting of transmembrane receptors into multivesicular bodies (MVBs) is a crucial feature of eukaryotic cell biology because of its ability to regulate signal transduction. Since active signaling is transduced via the cytoplasmic domain of the receptor, topologically, signaling can still occur after internalization and delivery to early endosomes. It is only after receptor sequestration into intralumenal vesicles (ILVs) during MVB biogenesis that the signaling domain is removed from the cytosol and signal transduction is arrested. Sorting to MVBs is followed by fusion to lysosomes in which the final degradation of receptors and other sorted cargoes now embedded in ILVs occurs.

In yeast, genetic and biochemical evidence indicates that sorting of cargoes to ILVs is regulated by monoubiquitylation and by the function of the Hrs-STAM complex and three endosomal sorting complexes required for transport (ESCRT-I, ESCRT-II, ESCRT-III) (reviewed by Hurley and Emr, 2006). In this organism, mutation of components of either the Hrs-STAM complex (sometimes referred to as ESCRT-0) or the ESCRT-I, ESCRT-II, ESCRT-III complexes leads to similar exclusion of cargoes from the lumen of the vacuole, the yeast lysosome. These mutations result in formation of an aberrant 'class E' endosomal compartment characterized by extensive tubulation and absence of ILV-containing MVBs, indicating that that Hrs-STAM and ESCRT complexes are similarly required for MVB biogenesis (Raymond et al., 1992; Vida et al., 1993; Rieder et al., 1996; Babst et al., 2002; Bilodeau et al., 2002).

By contrast, in mammalian cells, studies using RNAi knockdown have provided a less consistent picture of the functions of Hrs-STAM and ESCRT-I, ESCRT-II, ESCRT-III in MVB biogenesis. In mammalian cells depleted of Hrs, endosomes are enlarged, MVBs are less abundant and contain a reduced number of internal vesicles (Razi and Futter, 2006). In cells depleted of the ESCRT-I component Tsg101, MVBs are not formed and are replaced by tubulated and multilamellar structures reminiscent of the yeast class E compartment (Doyotte et al., 2005; Razi and Futter, 2006); Finally, in cells depleted of the ESCRT-III component Vps24, MVBs are formed but they are smaller than those found in wild-type (WT) cells (Bache et al., 2006).

Although little studied at the ultrastructural level, work in *Drosophila* has shown that metazoan ESCRT activity can influence an unexpected range of developmental processes (Lloyd et al., 2002; Jekely and Rorth, 2003; Moberg et al., 2005; Thompson et al., 2005; Vaccari and Bilder, 2005; Herz et al., 2006). For instance, the ESCRT-I component Tsg101 and the ESCRT-II component Vps25 were found to act as neoplastic tumor suppressors (TSGs), controlling both polarity and proliferation of epithelial cells. In mutant cells, failure to degrade Notch and downregulate its signaling

Journal of Cell Science

Journal of Cell Science

promotes proliferation non-autonomously. The cargoes associated with Notch-independent phenotypes such as loss of cell polarity, cell-autonomous enhancement of proliferation, and activation of apoptosis have not been identified.

Whether these and other developmental functions in metazoans require all ESCRT components remains an open question. For example ESCRT-I, ESCRT-II and ESCRT-III components but not Hrs are required to prevent ectopic Notch signaling activation in *Drosophila* (Lloyd et al., 2002; Jekely and Rorth, 2003; Moberg et al., 2005; Thompson et al., 2005; Vaccari and Bilder, 2005; Herz et al., 2006; Vaccari et al., 2008). In addition, ESCRT-I and ESCRT-III, but not ESCRT-II, appear to be required at the plasma membrane for HIV virus budding and for the final step of cytokinesis in mammals (Martin-Serrano et al., 2003; Morita et al., 2007; Carlton et al., 2008). Finally, ESCRT proteins have also acquired novel functions in metazoans that appear unrelated to their role in protein degradation and MVB biogenesis. This is the case for the regulation of anterior mRNA localization in *Drosophila* oocytes, a function specific to ESCRT-II components (Irion and St Johnston, 2007).

In summary, recent evidence indicates that metazoan ESCRT proteins function in processes other than degradation of ubiquitylated proteins and MVB biogenesis and that some of these processes might be regulated by specific ESCRT complexes. Even during protein degradation and MVB biogenesis, it is currently unclear whether metazoan ESCRT complexes act as part of a single pathway, as in they do in yeast. The study of the cell biological and developmental role of ESCRT complexes in metazoans has, to date, been hampered by the difficulty in analyzing tissues and cells completely lacking function of each ESCRT component. Indeed, ultrastructural and signaling analyses in mammals have relied mostly on knockdown approaches, and in only a few cases have developmental studies in *Drosophila* been conducted using null mutants. Identification and comparative analysis of null mutants in all of the ESCRT genes will be required for full elucidation of the repertoire of metazoan ESCRT-regulated processes. Here, we report the identification and initial comparative genetic, cell biological and developmental characterization of null mutations in five novel *Drosophila* ESCRT genes, belonging to the ESCRT-I, ESCRT-II and ESCRT-III complexes. Our analyses highlight an additional cell biological role of ESCRT proteins in *Drosophila*, and suggest that the role of ESCRT-III in some ESCRT-mediated processes differs from that of ESCRT-I and ESCRT-II.

Results

Efficient genetic screening identifies mutants that disrupt novel ESCRT genes

To systematically isolate mutations disrupting *Drosophila* ESCRT components, we first identified the homologs of each yeast ESCRT-encoding gene in the fly genome. In yeast, the three ESCRT complexes are composed of a total of eleven proteins. In *Drosophila*, a single gene encoding homologs of each of these components exists, with the exception of *vps37* for which two homologs can be found. Four ESCRT homologs map to chromosome arm 2R and 3R, two to X and 3L and none to 2L (Table 1). Since chromosomes 2R and 3R contain the most predicted ESCRT genes, we devised a screening strategy to isolate ESCRT mutations on these chromosome arms. We exploited the fact that when larvae contain eye imaginal discs that are completely composed of cells mutant for the ESCRT-I component *tsg101* or the ESCRT-II component *vps25*, a distinctive 'giant larvae' phenotype results (Moberg et al., 2005; Thompson et al., 2005; Vaccari and Bilder, 2005). These animals are blocked in pupation and do not eclose as adults; we refer to this phenotype as 'mutant eyes, no eclosion' (MENE) and have recently described an efficient screen on chromosome 2L and 3R for MENE mutations (Menut et al., 2007). We therefore used the same genetic strategy to isolate MENE mutations on chromosome 2R to test whether ESCRT mutations on this chromosome arm could be identified. Statistics of the MENE mutations recovered in the 2R screen are presented in Table 2.

ESCRT mutant tissue in *Drosophila* displays a cell-autonomous loss of polarity and growth control (Moberg et al., 2005; Thompson et al., 2005; Vaccari and Bilder, 2005). Such neoplastic tumor suppressor gene (TSG) behavior results in the formation of overgrown and disorganized imaginal discs that express high levels of cortical actin and of matrix metalloprotease 1 (MMP-1) (Menut et al., 2007). Thus, to identify putative ESCRT mutants in our 2R MENE collection, we first immunostained mutant discs to detect actin and MMP-1 (supplementary material Fig. S1; and data not shown). We found that seven MENE mutants falling into five complementation groups, named *MENE(2R)A-E,* displayed a neoplastic tumor suppressor phenotype (supplementary material Fig. S1C-H; Table 2). We have previously reported the characterization of *MENE(2R)D*, which disrupts the ESCRT-II component *vps25* (Vaccari and Bilder, 2005). Not including *MENE(2R)D/vps25*, together, the screen reported here and that of Menut and colleagues (Menut et al,. 2007) establish a collection

Table 1. Conservation of ESCRT genes in Drosophila

Complex	Yeast homologs	Fly gene name	CG number	Chromosome arm	Cytology	Reference
ESCRT-I	Mvb12a	–	7192	X	16F6	–
	Vps23/Stp22	*Erupted/tsg101*	9172	3L	73D1	(Moberg et al., 2005)
	Vps28	*Dvps28*	12770	2R	44A4	This study; (Sevrioukov et al., 2005)
	Vps37	*vps37A/mod(r)*	17828	X	1B12	–
		vps37B	1115	3R	82F6	–
ESCRT-II	Vps22	*larsen/vps22*	6637	3R	93F14	This study; (Irion and St Johnston, 2007)
	Vps25	*vps25*	14750	2R	44D4	This study; (Thompson et al., 2005; Vaccari and Bilder, 2005; Herz et al., 2006)
	Vps36	–	10711	3L	70B4	–
ESCRT-III	Vps2/Did4	–	14542	3R	96F10	This study
	Vps20	–	4071	2R	58F2	This study
	Vps24	–	9779	3R	82A4	–
	Vps32/Snf7	*shrub*	8055	2R	45A12	This study; (Sweeney et al., 2006)

Table 2. MENE (2R) screen

Statistics					
Number of crosses	Number of mutant chromosomes (estimated)		Number of MENE alleles		Initial hit (%)
10541	6662		98		1.5
Phenotypic classes					
No defect	Class Ia (hyperplastic)*	Class Ib (nTSGs)†	Class II (other)‡	Class III (small disc)§	Class IV¶
16 alleles	4 alleles	10 alleles	16 alleles	38 alleles	14 alleles
Class Ib mutants					
Complementation group				Number of alleles	
MENE (2R)-A				3 (*A2*, *B9*, *D2*)	
MENE (2R)-B				1 (*I3*)	
MENE (2R)-C				2 (*G5*, *O3*)	
MENE-D (*vps25*)				1 (*A3*)	
MENE (2R)-E				1 (*B6*)	
MENE (2R)-F				2 (*C5*, *O9*)	

*See B15 in supplementary material Fig. S1.
†See MENE (2R) in supplementary material Fig. S1.
§See I17 in supplementary material Fig. S1.
§See A16 in supplementary material Fig. S1.
¶Inconsistent defect or not determined.

of mutations that disrupt 12 uncharacterized neoplastic TSGs on chromosome 2R and 3R, possibly including novel ESCRT components.

To identify mutations within this collection that might disrupt genes encoding ESCRT proteins, we then tested the ability of the newly identified mutations to affect non-autonomous growth, which occurs in the ESCRT mutants *tsg101* and *vps25* but not other identified neoplastic TSG mutants (Moberg et al., 2005; Thompson et al., 2005; Vaccari and Bilder, 2005). Non-autonomous overgrowth can be assessed by generating genetically mosaic eye discs containing both WT and mutant cells, rather than discs composed exclusively of mutant cells as was done in the MENE screen (Fig. 1). In these discs, cells mutant for non-ESCRT neoplastic TSGs, such as *avalanche* (*avl*), were eliminated by cell competition (Fig. 1B). The resulting adult eyes were grossly morphologically normal and contained all WT ommatidia (Fig. 1B′). By contrast, complementation groups *MENE(2R)-A* to *MENE(2R)-C*, *MENE(3R)-A* and *MENE(3R)-E* showed a distinct phenotype: homozygous mutant tissue partially survived in the context of mosaic eye discs (Fig. 1C-H); this phenotype was most pronounced in *MENE(2R)-A, MENE(2R)-B* and *MENE(3R)-A* mutants. In addition, although mutant ommatidia were not recovered in any of

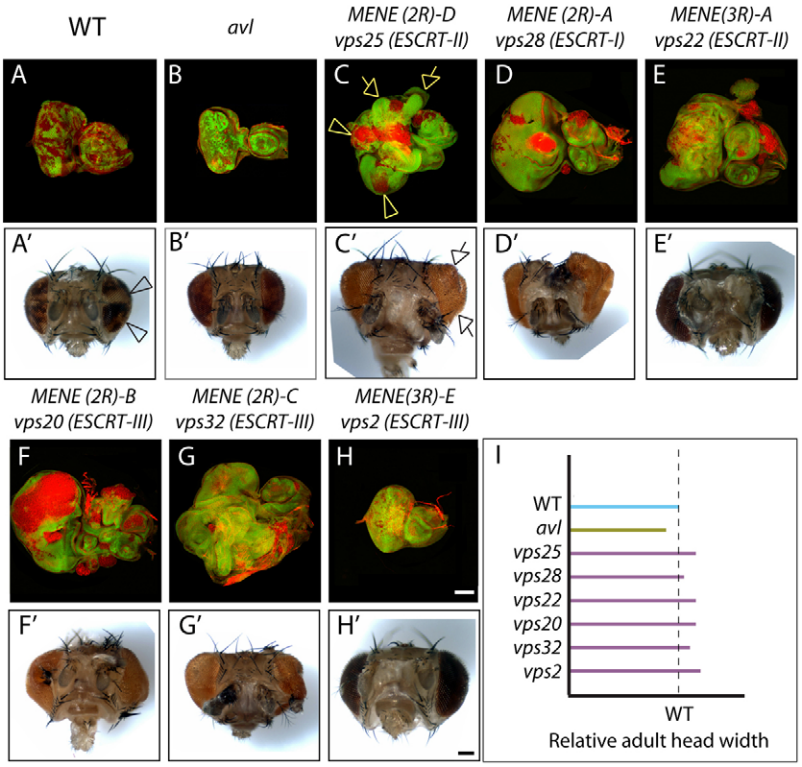

Fig. 1. Neoplastic TSG complementation groups that control proliferation non-autonomously. (A-H) Mosaic eye imaginal discs stained with phalloidin to detect cortical filamentous actin (F-actin; red). Mutant cells are marked by absence of GFP expression (green). In contrast to *avl* clones (B), cells mutant for ESCRT complementation groups *MENE(2R)-A* to *MENE(2R)-D* and *MENE(3R)-A, MENE(3R)-E* (C-H) survive and overproliferate to form disorganized masses of cells in the context of mosaic discs (arrowheads in C). In addition, the WT (GFP-positive) tissue surrounding ESCRT mutants overproliferates to generate extra folds of tissue within enlarged eye discs (arrows in C). Note that these phenotypes are less pronounced in *MENE(2R)-C/vps32/*ESCRT-III (G) and *MENE(3R)-E/vps2/*ESCRT-III (H). (A′-H′) Bright-field images of adult eyes deriving from mosaic eye discs corresponding to the same genotype as in A-H. Mutant chromosomes carry the red pigment defective allele *w*–, whereas WT chromosome carries *w*+. In contrast to control (A′ arrowhead), ommatidia composed of *w*– cells are not recovered, indicating that homozygous neoplastic TSG mutant cells do not contribute to the formation of adult eyes (B′-H′). Despite this, in contrast to control (A′) and to the adult eye of *avl* mosaic animals (B′), the adult eye of ESCRT mosaic animals is overgrown and bulging (arrowhead in C′), revealing variable levels of non-autonomous induction of proliferation (C′-H′). (I) Quantification of the adult head width of the mosaic animals in A′-H′ shows overgrowth in ESCRT mutants compared with WT control (dashed line). Scale bars: 100 µm.

Table 3. Sequencing of ESCRT mutations

Comp. Group	Gene	Complex	Allele	Mutation	Amino acid change
MENE (2R)-A	*vps28*	ESCRT-I	*A2*	111 bp deletion ...GAGTTGAGCGAGΔ	E186/211 → frameshift
			B9	16 bp deletion ...CGACTGCATTACΔ	I49/211 → frameshift
			D2	nonsense CGA → TGA	R102/211 → STOP
MENE (2R)-D	*vps25*	ESCRT-II	*A3*	(Vaccari and Bilder, 2005)	–
MENE (3R)-A (Menut et al., 2007)	*vps22*	ESCRT-II	*NN31*	nonsense CAG → TAG	Q137/254 → STOP
			SS6	nonsense AAG → TAG	K218/254 → STOP
			XX3	nonsense TGG → TGA	W238/254 → STOP
			ZZ13	nonsense TGG → TGA	W86/254 → STOP
MENE (2R)-B	*vps20*	ESCRT-III	*I3*	3′ splice nonsense TAG → TTG	K61/212 → frameshift
MENE (2R)-C	*vps32*	ESCRT-III	*G5*	384 bp deletion ...AGAAAAAGAAGCΔ	K69/226 → frameshift
			O3	85 bp deletion ...CGATGCCATTTCΔ	I145/226 → frameshift
MENE (3R)-E (Menut et al., 2007)	*vps2*	ESCRT-III	*PP6*	nonsense CAG → TAG	Q111/256 → STOP

For mutants containing point mutations, the mutated base is underlined. For mutants containing deletions, the nucleotide (nt) size of the deletion and the last 12 bases before the 5′ breakpoint are displayed. The last amino acid before the introduced stop codon or frame shift relative to the total size is displayed in the 'amino acid change' column. Based on the published structure of the ESCRT-I and II complexes (reviewed by Saksena et al., 2007), Vps28 truncations are predicted to lack part of the C-term domain that mediates recruitment of the ESCRT-II complex. For details about *vps25* see Vaccari and Bilder (Vaccari and Bilder, 2005). Vps22 truncations lack either Vps25 or Vps36 binding domains.

these genotypes, the WT ommatidia composing the adult eyes of mosaic animals were variably overgrown (Fig. 1C′-H′). These data indicate that, out of the collection of neoplastic TSG complementation groups, five display an ESCRT-like behavior.

To test whether these five complementation groups disrupt ESCRT loci, we performed complementation tests with chromosomal deficiencies that remove genes encoding ESCRT proteins on the appropriate chromosome arms. We found that all five complementation groups failed to complement such deficiencies, including those removing genes encoding the ESCRT-I component Vps28, the ESCRT-II component Vps22, and the ESCRT-III components Vps20, Vps32 and Vps2. Direct sequencing of the ESCRT coding sequences in the 12 non-complementing alleles revealed either nonsense mutations or deletions with one exception: *MENE(2R)-B* contained an altered 3′ mRNA splicing acceptor site in intron 2 of *vps20* (Table 3). All these mutations are predicted to cause premature translation termination. Because all ESCRT proteins are part of highly structured multicomponent complexes (Williams and Urbé, 2007), even if expressed, the resulting predicted truncated proteins are likely to disrupt formation of the corresponding complex. The molecular data therefore predict that each of the novel ESCRT mutants behaves as a functional null. Consistent with this assessment, lethal-phase analysis of the ESCRT alleles on chromosome 2R demonstrated that both animals homozygous for each mutant allele, and animals hemizygous for a chromosomal deficiency removing the locus, died as L1 larvae (data not shown).

We were surprised to isolate mutations in the ESCRT-I component *vps28* in the screen, since it has been reported that *vps28* mutant cells do not show cell polarity or proliferation phenotypes, nor do they alter delivery of proteins to the lysosome or MVB formation (Sevrioukov et al., 2005). In striking contrast, all three *vps28* alleles recovered in our screen caused neoplastic tumors (supplementary material Fig. S1C; and data not shown). To confirm that the phenotypes examined were due to loss of *Vps28* function, we performed a rescue experiment (supplementary material Fig. S2A-B). We found that imaginal disc cells mutant for the neoplastic *vps28* allele accumulated high amounts of ubiquitin (supplementary material Fig. S2A), whereas transgenic expression of WT Vps28 in mutant cells rescued both the cell architecture and ubiquitin degradation phenotypes (supplementary material Fig. S2B). These data confirm that *vps28* is indeed required for protein degradation and neoplastic tumor suppression, and suggest that the previously described *vps28* allele is a partial loss-of-function mutant.

All newly identified *Drosophila* ESCRT components sort ubiquitylated proteins and Notch

A major function of the yeast ESCRT proteins involves the endosomal sorting and degradation of ubiquitylated proteins. Mutations in *Drosophila tsg101* (ESCRT-I) and *vps25* (ESCRT-II) lead to endosomal ubiquitin accumulation; we therefore tested whether the additional *Drosophila* ESCRT proteins identified in the screen are required for trafficking and degradation of ubiquitylated cargo (Moberg et al., 2005; Thompson et al., 2005; Vaccari and Bilder, 2005; Herz et al., 2006). We generated mosaic eye discs containing clones of mutant cells for *vps28* (ESCRT-I), *vps22* (ESCRT-II), *vps20*, *vps32* and *vps2* (ESCRT-III) and immunostained them to detect ubiquitin. We found that, in contrast to the WT, in which no ubiquitin signal was detected because of the high rate of degradation of ubiquitylated cargo, all ESCRT mutants tested displayed severe intracellular ubiquitin accumulation (Fig. 2A-F). These data demonstrate that all three *Drosophila* ESCRT complexes are required for degradation of ubiquitylated proteins.

In addition to accumulating ubiquitylated proteins, tissue mutant for the ESCRT-I, ESCRT-II and ESCRT-III components

Journal of Cell Science

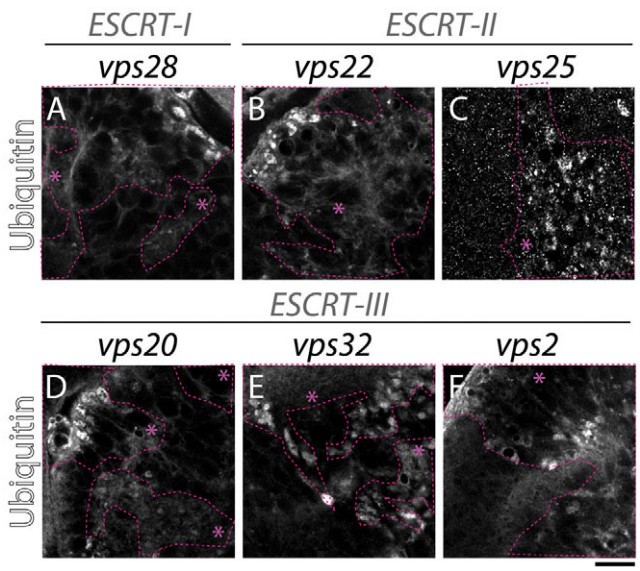

Fig. 2. ESCRT complexes are required for degradation of ubiquitylated proteins. ESCRT-I (A), ESCRT-II (B,C) and ESCRT-III (D-F) mosaic eye discs stained with anti-ubiquitin. Compared with the WT tissue, ubiquitin accumulates in intracellular puncta in clones of mutant cells, indicating failure of degradative MVB sorting. Clones are encircled with dashed pink lines and marked with an asterisk. Scale bar: 10 µm.

tsg101, *vps25* or *vps20* fails to degrade the signaling receptor Notch (Moberg et al., 2005; Thompson et al., 2005; Vaccari and Bilder, 2005; Herz et al., 2006; Vaccari et al., 2008). In mutant cells, undegraded Notch accumulates in enlarged endosomes that can be labeled by immunostaining for the endosomal syntaxin Avl (Vaccari and Bilder, 2005). Thus, we assessed whether Notch accumulates in enlarged endosomes in cells lacking Vps28 (ESCRT-I), Vps22 (ESCRT-II), Vps32 or Vps2 (ESCRT-III). All mutants except for one showed a similar accumulation of Notch in enlarged Avl-positive endosomes (Fig. 3A-F). Interestingly, cells mutant for *vps32* displayed lower amounts of accumulated Notch than cells mutant for other ESCRT components (Fig. 3F). We conducted a more extensive analysis of Notch accumulation in *vps32* mutant tissue, using antibodies directed to its extracellular domain on both fixed and cultured live tissue. In both cases, Notch accumulation was much less prominent in endosomes of *vps32* mutants than in *vps25* mutants, and in *vps32* mutants, a subset of Notch appeared to be redistributed to the cell cortex (Fig. 3G,L). These data point to a different role for *vps32* in Notch trafficking, and suggest that in *vps32* mutants either less Notch is internalized and fails to be degraded, or that some Notch can escape endosomal trapping.

Intracellular Notch accumulation in *tsg101* and *vps25* mutants correlates with ectopic Notch signaling activation (Moberg et al., 2005; Thompson et al., 2005; Vaccari and Bilder, 2005; Herz et al., 2006; Vaccari et al., 2008). Consistently, all ESCRT protein mutants tested displayed ectopic expression of Unpaired, a specific Notch target (Fig. 3M-R), although *vps32* cells show lower amounts of ectopic Unpaired. In addition, all ESCRT mutants tested also ectopically express *m*β-*lacZ,* a reporter for Notch signaling activity (data not shown). These data indicate that ESCRT-I, ESCRT-II, ESCRT-III components are required to control Notch signaling activation, also reflected by their ability to promote non-autonomous proliferation (Fig. 1).

All newly identified *Drosophila* ESCRT components downregulate EGFR, restraining its signaling potential

Mammalian cell studies have shown that degradation of the epidermal growth factor receptor (EGFR) is impaired when ESCRT function is reduced via RNAi (Kanazawa et al., 2003; Doyotte et al., 2005; Komada and Kitamura, 2005; Razi and Futter, 2006). EGFR accumulation leads to sustained levels of signaling activation in cells depleted of ESCRT-I and ESCRT-II components, but interestingly, not ESCRT-III components (Babst et al., 2000; Bache et al., 2006). In *Drosophila* embryos mutant for *hrs,* EGFR degradation was also reduced and signaling was enhanced (Lloyd et al., 2002), but the role of *Drosophila* ESCRT components in regulating EGFR has not been assessed. To examine how complete lack of ESCRT-I, ESCRT-II or ESCRT-III function affects EGFR degradation in *Drosophila*, we stained mosaic eye discs containing ESCRT mutant cells using an antibody against EGFR. In eye discs containing ESCRT mutant cells, some EGFR can be detected in intracellular puncta (Fig. 4A-E). These puncta also contain Notch, indicating that both receptors accumulate in the same endosomal compartment and suggesting that EGFR degradation is reduced in flies mutant for ESCRT-I, ESCRT-II and ESCRT-III proteins.

To determine whether lack of ESCRT components alters EGFR signaling, we stained mosaic eye discs containing ESCRT mutant cells using an antibody against the EGFR signaling component *capicua* (*cic*), whose nuclear expression levels are downregulated upon EGFR signaling activation (Tseng et al., 2007). We found that mutant cells showed lower nuclear Cic expression than surrounding WT cells, indicating that ESCRT activity is required to downregulate EGFR signaling (Fig. 4F-J). In addition, we assessed genetic interactions between ESCRT and EGFR pathway mutants, using Elp^{B1}, a hypermorphic EGFR allele in which signaling overactivation induces formation of ectopic wing veins (Baker and Rubin, 1989). Consistent with the Cic data, we found that the Elp^{B1} oversignaling phenotype is dominantly enhanced by ESCRT null alleles. It is also dominantly enhanced by mutants of the endosomal syntaxin *avl*, which regulates endosomal cargo entry (Fig. 4K-M). Overall, these data indicate that endocytosis, including MVB sorting by ESCRT-I, ESCRT-II and ESCRT-III complexes, is required for EGFR signaling downregulation in *Drosophila*.

ESCRT components are required for membrane stability and actin cytoskeleton stability in *Drosophila*

Recent evidence points to the possibility that ESCRT functions might have expanded to assume novel roles during metazoan development. To analyze roles of ESCRT during *Drosophila* oogenesis, we generated ESCRT-I, ESCRT-II and ESCRT-III null germline clones. We confirmed that null alleles of ESCRT-II (*vps25*) but not ESCRT–I (*vps28*) components show mislocalization of Staufen to the anterior oocyte pole, a germline ESCRT-II specific function independent of MVB sorting and biogenesis (supplementary material Fig. S2C-F) (Irion and St Johnston, 2007). These experiments showed that germline cells mutant for components of ESCRT complexes developed to late stages of oogenesis, indicating that ESCRT function is not essential for overall oocyte development (Fig. 5D). However, phalloidin staining revealed that ESCRT mutant germline cells frequently lacked subcortical actin, suggesting the presence of actin cytoskeleton defects (Fig. 5B,E-F,L). Similarly to the germline, *vps22* mutant follicle cells often appeared to lack subcortical actin (Fig. 5F-G). We then generated clones of *tsg101*

Journal of Cell Science

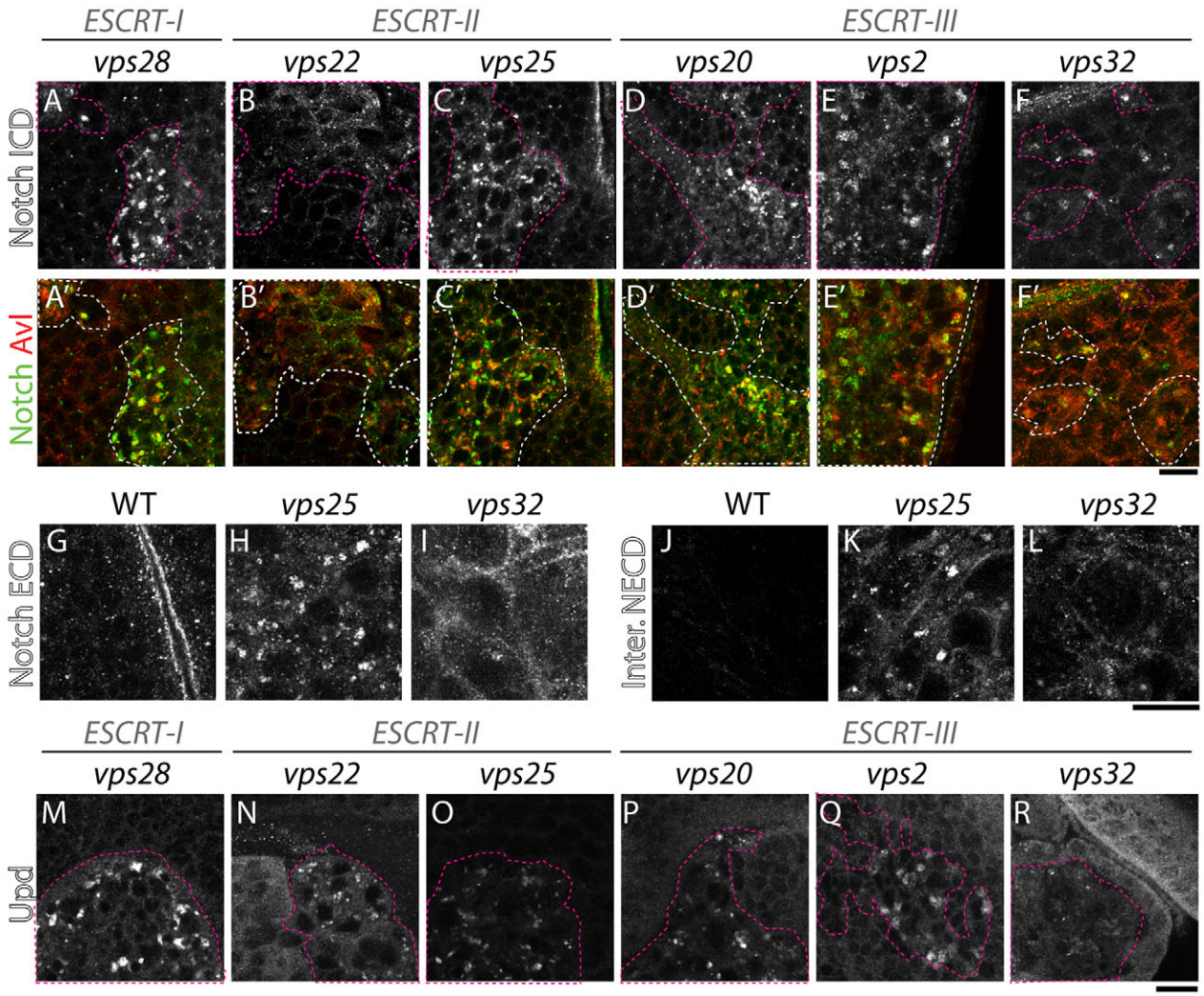

Fig. 3. Notch accumulates in endosomes of ESCRT mutant cells leading to overactivation of signaling. (A-F) ESCRT-I, ESCRT-II and ESCRT-III mosaic eye discs stained with an antibody recognizing the intracellular domain of Notch. Compared with WT tissue, Notch is depleted from the cellular surface and accumulates in enlarged endosomes (labeled Avl in A′-F′) in all ESCRT mutants except *vp32* mutants, in which less Notch accumulates (F). (G-L) Notch localizes in intracellular puncta in *vps25* mutants and is diffuse in *vps32* mutants. Notch immunodetection (Notch ECD; G-I) and 5 hour Notch internalization assay (inter. NECD; J-L) using antibodies directed to the extracellular portion of Notch in WT (G,J), *vps25* (H,K) and *vps32* (I,L) entirely mutant eye disc tissue. In *vps32* mutants, Notch accumulation in intracellular puncta is reduced, whereas cortical localization is increased compared with *vps25* (especially visible on fixed tissue in I). Note that in J, very little signal is present because most Notch is degraded 5 hours after labeling. (M-R) ESCRT-I, ESCRT-II and ESCRT-III mosaic eye discs stained with an antibody to detect expression of the Notch target unpaired (Upd). Compared with WT tissue, Upd is ectopically expressed to varying degrees in mutant cells. Notably *vps32* mutants appear to express the lowest amounts of Upd. Mutant tissue is encircled by dashed pink lines in A-F, M-R (white in A′-F′). Scale bars: 10 μm.

(ESCRT-I) mutant cells in eye imaginal discs and again detected defects in cortical actin cytoskeleton (Fig. 5H). To assess whether the lack of cortical cytoskeleton reflected plasma membrane defects that result in formation of multinucleated cells, we subjected cultured mutant egg chambers to incorporation of FM4-64, a lipophilic fluorescent dye. The absence of FM4-64 incorporation in many germline nuclei and the presence of fragmented membranes suggests a loss of plasma membrane integrity in ESCRT mutant cells (Fig. 5J). This ultimately led to the formation of clusters of multinucleated cells enclosed by a single actin cytoskeleton, whose nuclei rested around clumps of actin-positive structures, possibly also membrane fragments (Fig. 5L). Together, these data suggest that ESCRT-I, ESCRT-II and ESCRT-III function might be required for plasma membrane integrity and stability of the actin cytoskeleton.

Drosophila ESCRT-I and ESCRT-II, but not *hrs* or ESCRT-III components are required for MVB biogenesis

The isolation of null mutants in members of all three ESCRT complexes gave us the opportunity to directly assess the role of ESCRT proteins in metazoan MVB formation. In yeast, mutations in components of the ESCRT-I and ESCRT-III complexes, as well as in the *hrs* homolog, lead to a failure of MVB biogenesis, as assessed by absence of endosomes containing ILVs in ultrastructural analyses (Rieder et al., 1996; Babst et al., 2002; Bilodeau et al., 2002). By contrast, mammalian studies utilizing RNA knockdown concluded that although both Hrs and ESCRT-I proteins are required for MVB formation, ESCRT-III components are dispensable (Bache et al., 2003; Doyotte et al., 2005; Bache et al., 2006; Razi and Futter, 2006). To further investigate these differing findings in *Drosophila*, we utilized null mutants for *hrs* (Hrs-STAM), *tsg101* (ESCRT-I),

Journal of Cell Science

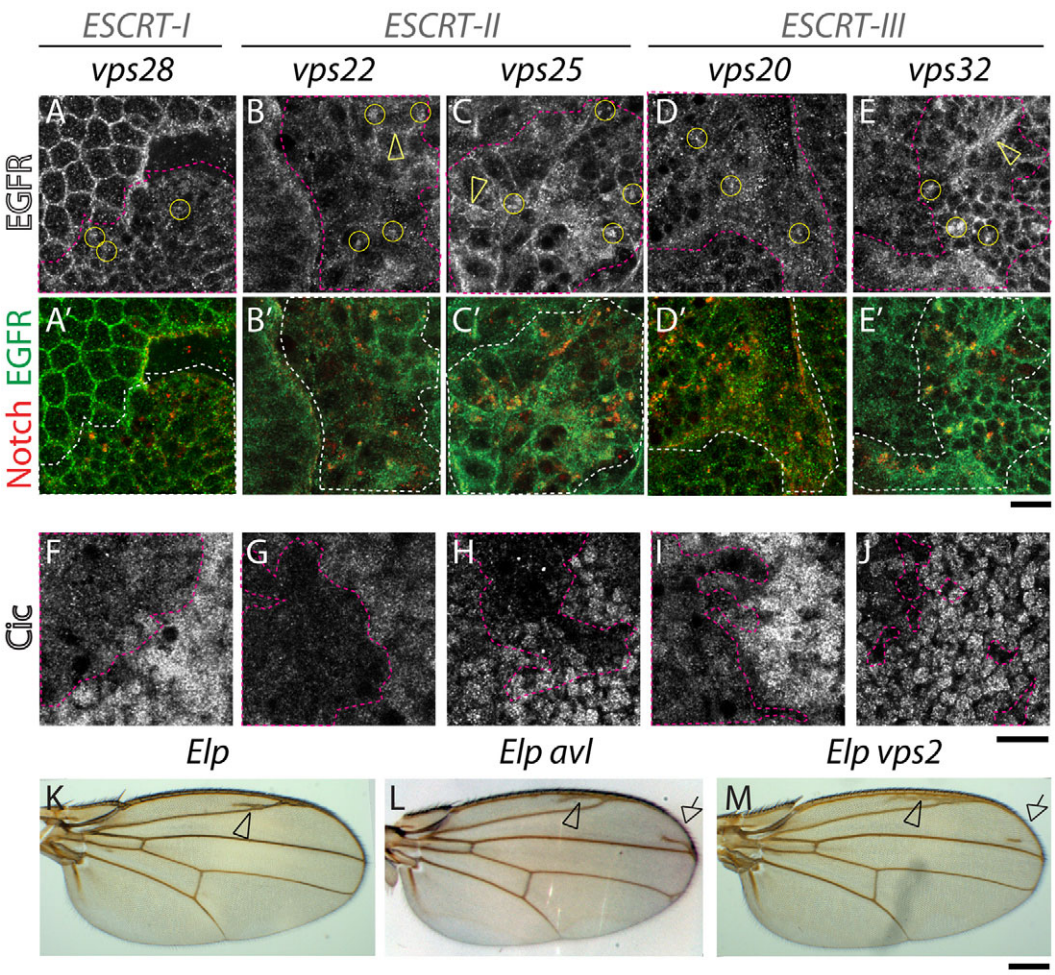

Fig. 4. EGFR accumulation and EGFR signaling is overactivated in ESCRT mutants. (A-E′) ESCRT-I, ESCRT-II and ESCRT-III mosaic eye discs stained with anti-EGFR (A-E) and Notch (merged in A′-E′); Compared with WT tissue, in mutant tissue (delimited by pink dashed lines) EGFR accumulation is seen in intracellular puncta (examples are encircled in A-E) that are Notch positive. Note that compared with Notch, the majority of EGFR is still detected in other cellular areas (arrowheads in B-C,E). (F-J) ESCRT-I, ESCRT-II and ESCRT-III mosaic eye discs stained with an antibody to detect expression of Capicua (Cic), a nuclear negative regulator of EGFR signaling. Compared with WT tissue, Cic expression is reduced in ESCRT mutant cells (delimited by pink dashed lines), indicating higher levels of EGFR signaling activation. Adult wings carrying *Ellipse* mutations, an activated form of EGFR (*Elp;* K). Animals also heterozygous for *avl* (*Elp avl*; L) or *vps2* (*Elp vps2*; M) show extra wing vein material, indicative of excessive EGFR signaling (arrowhead in K). The frequency of extra veins is increased in *Elp avl* wings (+82% *n*=60; arrows in L) and, to a lesser extent in *Elp vps2* (+38% *n*=19; arrows in L-M), indicating that excess EGFR signaling is enhanced by reducing endocytic gene dosage. Scale bars: 10 µm (A-J), 100 µm (K-M).

vps22 (ESCRT-II), and *vps20* and *vps32* (ESCRT-III) and tested whether ESCRT function is required for MVB formation in *Drosophila*. To this end, we analyzed endocytic compartments at the ultrastructural level in mutant oocytes, prepared by making germline clones (Fig. 6). Oocytes contain specialized endocytic compartments, called yolk granules, that mediate uptake of yolk proteins during vitellogenesis. During this process, most isolated MVBs fuse with yolk-containing endosomes to generate yolk granules that display a characteristic cortical population of ILV (Fig. 6A,B,H) (Schonbaum et al., 2000; Trougakos et al., 2001).

To identify the endocytic compartment and to follow yolk granule formation, we immunolabeled yolk proteins in ultrastructural preparations. In all mutant samples, labeling of yolk protein is still observed, indicating that yolk protein internalization, as expected, is not blocked in ESCRT mutants (Fig. 6C-G). We did not observe endosome tubulation, which is typical of yeast class E compartments, in any of the mutants. In oocytes mutant for *hrs*, yolk granules containing ILVs and isolated MVBs are present, although they are less abundant than in the WT; additionally, internalized yolk proteins are detected in regularly shaped yolk granules (Fig. 6C,H). This ultrastructural phenotype is consistent with a previous analysis of *hrs* mutant Garland cells (Lloyd et al., 2002), indicating that the endocytic phenotype observed in oocytes is not unusual or tissue-specific. However, in sharp contrast with *hrs*, in both *tsg101* (ESCRT-I) and *vps22* (ESCRT-II) mutant oocytes, yolk granules that contain ILVs and isolated MVBs are extremely rare (Fig. 6D,E,H). In addition to the near absence of all ILVs, *tsg101* and *vps22* oocytes also show irregularly shaped yolk granules (Fig. 6D-E). Remarkably, oocytes mutant for the ESCRT-III genes *vps32* or *vps20* appeared phenotypically more similar to those mutant for *hrs* than to *tsg101* or *vps22* mutants. Isolated MVBs and yolk granules containing ILVs could be detected in *vps32* and *vps20* mutant oocytes at frequencies that were similar to that of *hrs* mutants, and the yolk granules were regularly shaped (Fig. 6F,G, H). Together, these data suggest that MVB formation is not completely impaired in cells lacking at least two of the four ESCRT-

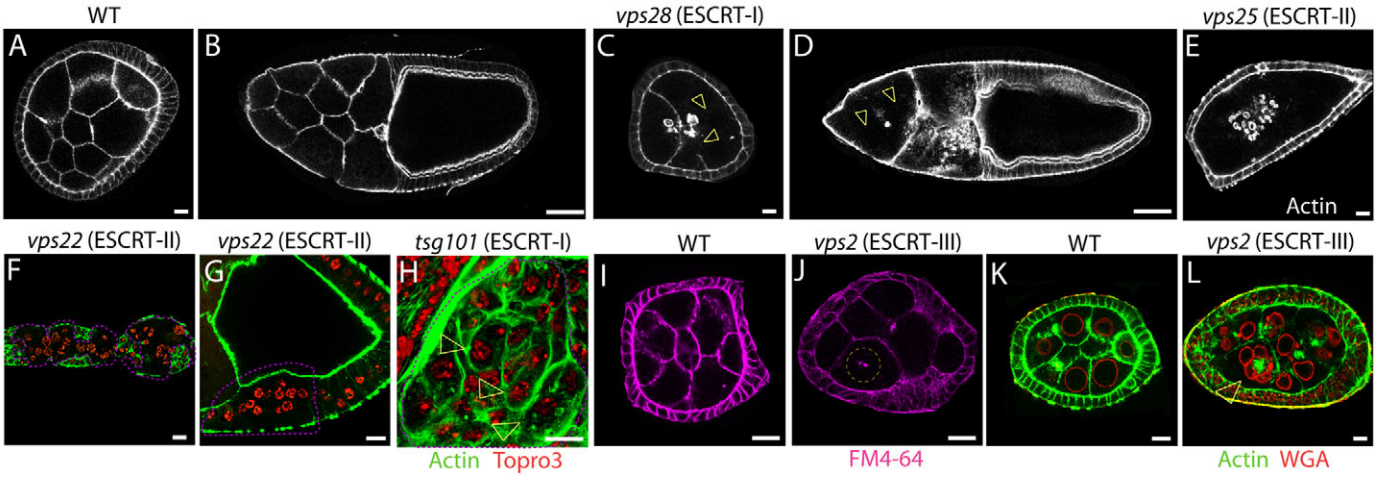

Fig. 5. ESCRT complexes regulate actin cytoskeleton stability and membrane integrity. (A-E) Stage 6 (A,C,E) and stage 10 (B,D) egg chambers stained with phalloidin to reveal the cortical actin cytoskeleton. Compared with WT (A,B), egg chambers containing *vps28* (ESCRT-I) and *vps25* (ESCRT-II) mutant germline cells (C-E) display varying degree of loss of cortical actin cytoskeleton (arrowhead in C-D). (F,G) Germarium and stage 1 egg chamber (F) and follicle cells overlaying a stage 9 egg chamber mutant for the ESCRT-II component *vps22* (delimited by the pink dashed line) display similar F-actin defects. (H) Eye imaginal disc cells mutant for the ESCRT-I component *tsg101* (delimited by the pink dashed line) display increased F-actin staining compared with surrounding WT cells. Despite this, loss of cortical actin cytoskeleton is observed, leading to clusters of two nuclei surrounded by a single actin cytoskeleton (arrowheads in H). In F-H cells are counterstained with Topro3 to visualize the nuclei. (I-L) Stage 6 egg chambers containing WT (I, K) or *vps2* (ESCRT-II) (J,L) mutant germline cells treated with FM4-64, a lipophylic dye that fluoresces upon membrane incorporation (I-J) or stained to detect F-actin and the nuclear membrane (WGA) (K,L). The plasma membrane dividing mutant cells appears incomplete (arrowhead in J), leading to the formation of multinucleated cells (arrowhead in L). Scale bars: 10 µm (A,C,E-L), 50 µm (B,D).

III components and indicate that in *Drosophila*, only ESCRT-I and ESCRT-II complexes are absolutely required for MVB formation.

Discussion

Current models of ESCRT function draw heavily from studies in yeast, where the complexes were first discovered and where they have been most completely analyzed. However, the straightforward paradigm from yeast – in which each component of the Hrs-STAM and ESCRT-I, ESCRT-II, ESCRT-III complexes acts primarily in MVB sorting and biogenesis – has been recently challenged by evidence in metazoans pointing to more diversified roles. Studies of metazoan tissues lacking each ESCRT component will be required to determine: (1) differences in ESCRT function between yeast and metazoans, (2) whether complexes and components always act together in a given cellular process, and (3) the complete set of processes that ESCRT genes regulate. Towards this goal we present here an efficient screening method to identify ESCRT mutations in *Drosophila*. The screen is based on the ability of ESCRT complexes to control tissue growth both autonomously and non-autonomously. Screening of three chromosome arms corresponding to approximately 60% of the *Drosophila* genome led to the identification of null alleles of five uncharacterized ESCRT genes, encoding components of all three ESCRT complexes. Our screen recovered alleles of all but two of the ESCRT homologs present on the chromosome arms screened. Mutations in the *vps24* homolog (ESCRT-III; *CG9779*) could not be recovered with the mosaic strategy used, because it lies proximal to the FRT used for screening. As for the second, *CG1115* (ESCRT-I) is one of the two *vps37* homologs present in the *Drosophila* genome; functional redundancy might mean that its inactivation alone does not induce overgrowth. We predict that execution of this screening strategy on chromosome arms X and 3L will further allow efficient identification of three of the remaining five ESCRT genes.

It is notable that the screen recovered no mutations in the *Drosophila hrs* or *stam* homologs, despite the fact that both genes lie on chromosome 2L distal to the FRT site with which we screened (Menut et al., 2007). In yeast, the Hrs-Stam complex has sometimes been referred to as 'ESCRT-0' because both *hrs* and *stam* mutants show identical disruption of trafficking and of endocytic compartmentalization to that of ESCRT-I, ESCRT-II or ESCRT-III mutants (Raymond et al., 1992; Bilodeu et al., 2002). However, existing *Drosophila hrs* mutants do not affect epithelial polarity, proliferation, or Notch signaling and ultrastructural data show distinct cell biological phenotypes for *hrs* and the ESCRT-I, ESCRT-II and ESCRT-III mutants analyzed in this work (Fig. 6) (Lloyd et al., 2002; Jekely and Rorth, 2003). Furthermore, mammalian RNA knockdown studies are consistent with different functions for the Hrs-Stam and ESCRT-I complexes (Sun et al., 2003; Razi and Futter, 2006). It is possible that functional redundancy between *hrs* and *stam* could explain the phenotypic difference between *Drosophila hrs* and ESCRT mutants, although we are not aware of any reports of redundant functions in the literature. An intriguing alternative possibility is that other proteins, perhaps the ESCRT-I complex, might functionally substitute for the metazoan Hrs-STAM complex. In agreement with this possibility, HIV-1 budding, a process topologically equivalent to ILV formation, is carried out by ESCRT-I and ESCRT-III components in the absence of Hrs-STAM function (Martin-Serrano et al., 2003); functional overlap might also be suggested by an earlier evolutionary origin for ESCRT complexes (Leung et al., 2008). A third possibility is that the Hrs-STAM complex acts in receptor protein degradation, but at a different step than other ESCRT complexes, one that is less crucial to control epithelial organization and Notch signaling. In either case, our results using null mutants in *Drosophila* highlight an important distinction between the function of ESCRTs and other ubiquitin-binding protein complexes in yeast and metazoans.

If ESCRT complexes do have a different role to the Hrs-STAM complex, how often do all three ESCRT complexes act together in a given cellular process? The identification of mutants in many

Journal of Cell Science

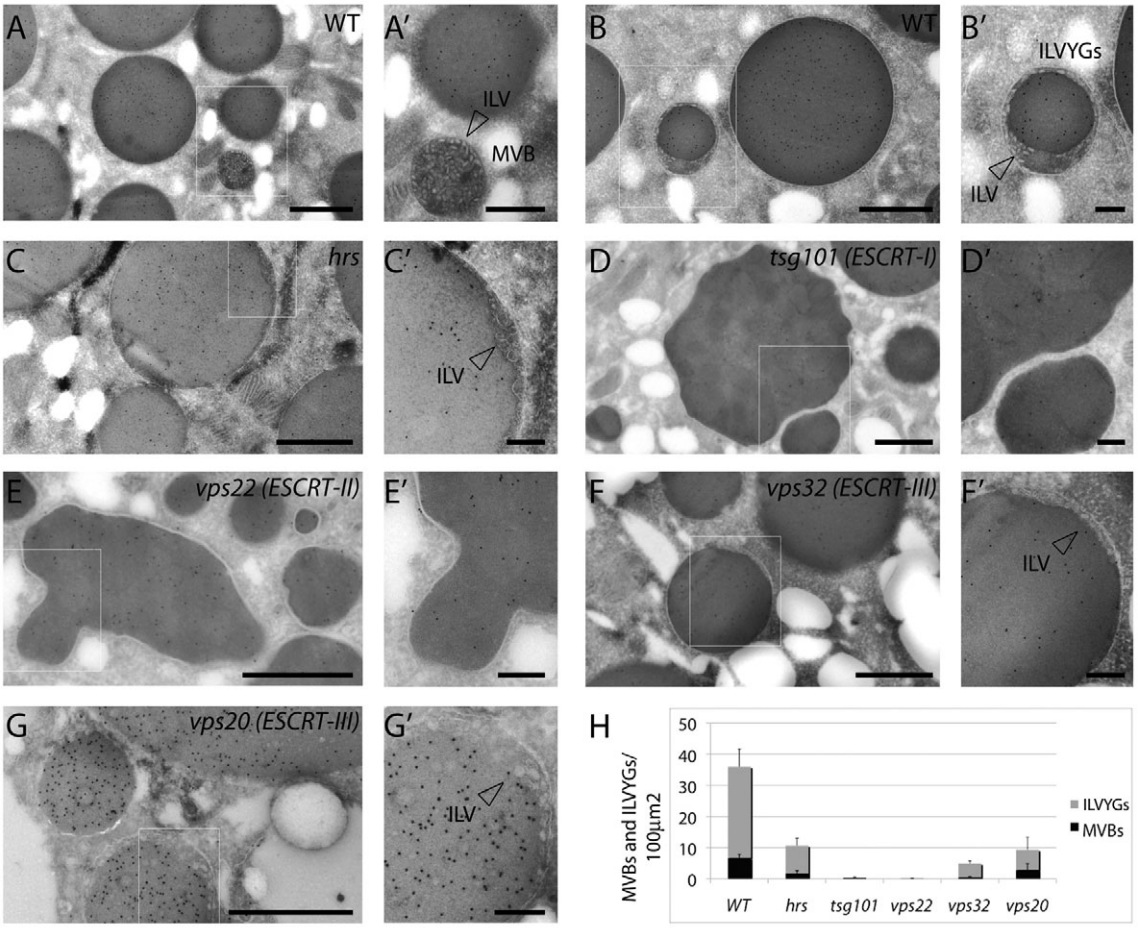

Fig. 6. Ultrastructural characterization of ESCRT-mutants. ESCRT-I, ESCRT-II but not *hrs* or ESCRT-III are crucial for MVB biogenesis. (A-G) Yolk protein immunolabeling with 10 nm gold particles on cryosections of *Drosophila* oocytes. WT stage 9-10 oocytes show accumulation of yolk proteins in the yolk granules (A). Isolated MVBs containing ILVs are also frequently observed in the ooplasm (A′). Additionally ILV-containing yolk granules (ILVYGs), derived from fusion with MVBs, are frequently observed (B). Magnification (B′) shows that ILVYGs contain ILVs. (C) In *hrs* (ESCRT-0) mutants, there is a similar phenotype, with presence of isolated MVBs and ILVYGs, although they are less abundant than in WT oocytes (arrowhead in C′ indicates ILV). (D) In the *tsg101* (ESCRT-I) mutants, the yolk granules still accumulate with large diameters; however, ILVYGs and isolated MVBs are absent. *vps22* (ESCRT-II) mutant oocytes (E) also lack ILVYGs and isolated MVBs. (D′-E′) Magnifications show lack of ILVs. Compared with WT, the *tsg101* and *vps22* yolk granules are irregularly shaped. (F,G) By contrast, the *vps32* and *vps20* (ESCRT-III) mutant oocytes possess regularly shaped ILVYGs as well as isolated MVBs, which are more similar to *hrs*. Scale bars: 1 µm (A-G), 0.25 µm (A′-G′). (H) Quantification of the number of ILVYGs and MVBs per 100 μm^2 in WT and mutant stage 10 ovaries. The number of ILVYGs and MVBs formed in the ESCRT-III mutants analyzed is similar to that of *hrs* mutant. By contrast, ESCRT-I and ESCRT-II mutant oocytes contains almost no ILVYGs and MVBs. Results are means ± s.d.

uncharacterized ESCRT genes provides a chance to explore this question by comparing the functions of the individual components and complexes. In most of the in vivo cellular and developmental assays we used, the ESCRT mutants closely resemble one another: they all cause autonomous neoplastic transformation, non-autonomous overproliferation (albeit to varying degrees), trap ubiquitylated proteins, and control stability of the actin cytoskeleton and membrane integrity. These data indicate that, as in yeast, *Drosophila* ESCRT complexes work together as a single functional unit to regulate these processes.

The existence of process-specific roles for individual ESCRT complexes in mammalian cells has been inferred by RNAi, which causes only a partial depletion of gene product. For instance, depletion of several ESCRT-I and ESCRT-II components but not the ESCRT-III component *vps24* by RNAi impairs EGFR degradation and signaling (Bache et al., 2006). This contrasts with our results using null alleles, which suggest that control of EGFR signaling is not a function where ESCRT components have different roles. Indeed, our data indicate a partial failure to degrade EGFR and upregulation of EGFR signaling in mutants for all of the ESCRT-III components examined. We have not yet analyzed *vps24* mutant cells (owing to its cytological location, as mentioned above), and it cannot be ruled out that functions of fly and mammalian ESCRT-III in EGFR degradation might differ. However, our analysis of *vps28* illustrates the importance of distinguishing null and hypomorphic situations. The previously studied *vps28* allele behaved as a strong hypomorph in genetic tests and almost no protein product could be detected in mutant tissue (Sevrioukov et al., 2005); the distinct trafficking, ultrastructural and developmental phenotypes of this allele raised the possibility that Vps28 had functions distinct from other ESCRT components. However, our isolation and analysis of true molecular null mutants reveals that the phenotype of *vps28* is indeed identical to other ESCRT-1 components, underlining the value of null alleles in reaching definitive conclusions about ESCRT function.

Nevertheless, we have noted consistent differences amongst null ESCRT component phenotypes, which interestingly all concern ESCRT-III components. In one example, *vps2* mosaic discs are less overgrown than other ESCRT mutant discs, both because the mutant clones are smaller and because less non-autonomous growth is present compared with other ESCRT mutants. Similarly, *vps32* clones grow less than *vps20* clones but, in this case, non-autonomous growth is as strong as in *vps20* mosaic eyes. In addition, cells lacking the ESCRT-III component Vps32 displayed less endosomal accumulation of Notch and more plasma membrane localization than other ESCRT mutants, suggesting that either Notch escapes endosomal trapping or that Vps32 is also required for initial internalization. Differential trapping of Notch might affect the extent of its ectopic activation.

Most unexpectedly, although oocytes mutant for ESCRT-I or ESCRT-II components display almost no endocytic compartments that contain ILVs, oocytes mutant for the ESCRT-III components *vps32* and *vps20* still display ILV-containing endocytic structures, albeit at a reduced frequency. This is in strong contrast to yeast, where the best-characterized role of yeast ESCRT proteins is in the formation of ILV-containing MVBs. Although we cannot absolutely rule out differential effects on protein stability in our germline clones, this would seem to be an unlikely explanation for the different phenotypes we observe (see Materials and Methods). Instead, these findings might suggest that the ESCRT-III complex acts slightly differently than ESCRT-I and ESCRT-II in controlling protein degradation and MVB biogenesis. Interestingly, two recent reports find that Vps32 homologs form oligomeric filaments that might either inwardly invaginate the endosomal membrane during MVB biogenesis, retain cargoes within these invaginations, or perform both functions (Hanson et al., 2008; Teis et al., 2008). The fact that at least two *Drosophila* ESCRT-III components appear dispensable in part for MVB formation, together with the reduced accumulation of Notch and cell-autonomous and non-autonomous proliferation of certain ESCRT-III mutants, when compared with ESCRT-II mutants, indicate that in *Drosophila*, the ESCRT-III complex might be more crucial for cargo retention than endomembrane invagination.

In the data discussed above we tested known or expected functions of ESCRT proteins. However, the isolation of many ESCRT mutants also provides the opportunity to search for novel functions, one of which we describe here that is common to all the ESCRT genes. Cells mutants for any ESCRT component show strong defects in actin and plasma membrane organization. ESCRT complexes might directly regulate the actin cytoskeleton, as previously suggested (Sevrioukov et al., 2005). However, we also detected a failure to incorporate lypophilic dyes into the plasma membranes of ESCRT mutant cells. This suggests that the loss of cortical actin and loss of plasma membrane might be related, ultimately leading to the formation of multinucleated cells. Recent reports have demonstrated that mammalian ESCRT components interact with midbody proteins and control the last steps of cytokinesis, a process topologically similar to HIV and exosome budding from the plasma membrane and endomembrane invagination during MVB formation (Morita et al., 2007; Carlton et al., 2008). This raises the possibility that defective cytokinesis might account for the presence of multinucleated cells in *Drosophila* ESCRT mutants. However, we also observed these defects in cells lacking ESCRT-II components, which are dispensable for cytokinesis in mammalian cells, suggesting that the actin and plasma membrane organization might not be a consequence of aberrant cytokinesis. In addition, knockdown of several ESCRT components in *Drosophila* tissue culture cells does not lead to high proportion of multinucleated cells (data not shown). Interestingly, the germline phenotype of ESCRT mutants is reminiscent of that reported for cells lacking the exocytic trafficking proteins Sec5 and Rab6 and the recycling component Rab11 (Murthy and Schwarz, 2004; Bogard et al., 2007; Coutelis and Ephrussi, 2007). Thus, we raise the possibility that ESCRT complexes might also have a role in stabilizing the plasma membrane and its underlying actin cytoskeleton during membrane growth after cell division, a process particularly crucial during egg chamber development. Future work will be required to evaluate this potentially underappreciated role of ESCRT in membrane stabilization.

In conclusion, our identification and initial comparative genetic, cell and developmental analysis of null mutants for nearly half of the ESCRT genes encoded by the *Drosophila* genome refines the current understanding of their role in degradation of ubiquitylated proteins and MVB biogenesis. It also clarifies previous contrasting evidence on ESCRT function in yeast, *Drosophila* and mammals. Finally, it uncovers a novel developmentally relevant role for ESCRT genes. Future use and expansion of the toolbox of *Drosophila* null ESCRT mutants reported here will pave the way to the elucidation of the full repertoire of metazoan-specific ESCRT-dependent processes, and those that are common to all complexes as well as those that are complex- or component-specific.

Materials and Methods

Genetics and fly stocks

EMS screening was conducted using isogenized stocks of *w; FRT42*. The MENE screen on 2R utilized the line *yw eyFLP; cl [w+] FRT42/CyO TwiGal4 UAS-GFP* (Newsome et al., 2000). *Gla/CyO TwiGal4 UAS-GFP* was used to balance and stock mutant chromosomes. *yw;; eyFLP cl GMR-hid FRT82/TM6C* was used to generate entirely mutant eye discs for 3R ESCRT mutants. To generate mosaic eyes we used *yw eyFLP; ubiGFP[w+] FRT42* and *yw eyFLP; ubiGFP FRT82* (Tapon et al., 2001) and for mosaic wing discs, *UbxFLP; ubiGFP[w+] FRT42/Cyo* (Hong et al., 2003). We utilized *hsFLP; armLacZ FRT42* (Bloomington), and *hsFLP OvoD FRT40, 80* and *82* lines to generate germline clones (Chou et al., 1993). Other alleles utilized were: $tsg101/ept^{2}$, $vps25^{A3}$, avl^{1}, hrs^{D28} (Lloyd et al., 2002; Lu and Bilder, 2005; Moberg et al., 2005; Vaccari and Bilder, 2005).

EMS mutagenesis

Male flies carrying an isogenized *FRT* chromosome were starved for 8 hours and subsequently fed a 25 mM EMS solution overnight at room temperature. To screen the 2R chromosome arm, mutagenized *FRT42* males were mated en masse to *Gla/CyO TwiGal4 UAS-GFP* females. Single F1 males of the genotype **FRT42/Cyo TwiGal4 UAS-GFP* were each crossed to three females of the genotype *eyFLP cl FRT42/CyO TwiGal4 UAS-GFP*. Absence of non-*CyO* adults in the F2 progeny indicated a positive MENE phenotype. Mutant chromosomes were then recovered by crossing F2 males of the genotype **FRT42/Cyo TwiGal4 UAS-GFP* to *Gla/Cyo TwiGal4 UAS-GFP* females.

Immunohistochemistry, FM4-64 incorporation and confocal microscopy

Fixation was performed at room temperature for 20 minutes in a methanol-free, 4% paraformaldehyde solution. Actin staining was done using TRITC-conjugated phalloidin 1:500 (Sigma). Before antibody staining samples were incubated in a blocking solution of 5% normal goat serum. Primary antibody stains were done at 4°C overnight, and secondary antibody stains were done at room temperature for 2 hours. Primary antibodies to the following antigen were used: Notch ICD, Notch ECD (1:50; both from DSHB), Ubiquitin (FK2 1:1000; Biomol). Secondary antibodies used were conjugated Alexa Fluor 488 and Alexa Fluor 647 from Molecular Probes. Notch internalization was performed as described (Vaccari et al., 2008). For FM4-64 (Molecular Probes) incorporation, ovaries were dissected in S2 cell medium (Sigma) and incubated in medium containing 10 μM FM4-64 for 5 minutes at room temperature, washed in fresh medium, mounted and imaged. All images are single confocal sections taken with a TCS microscope (Leica) using 16× NA0.5, 40× NA1.25 or 63× NA1.4 oil lenses. Images were edited with Adobe Photoshop CS and were assembled with Adobe Illustrator 10.

Transmission electron microscopy

To minimize protein perdurance in germline clone analysis, we analyzed stage 10 oocytes from females at least 1 week old. Because the germline originates from a single stem cell, the analyzed tissue corresponds approximately to at least 10 days after gene inactivation and an expected 10^4 dilution of the original protein

Journal of Cell Science

concentration because of increasing cytoplasmic volume (D.B. unpublished and Kevin Kolahi and Anne K. Classen, University of California, Berkeley, CA, personal communication). Dissected ovaries were immediately transferred to fixative containing 4% formaldehyde and 0.1% glutaraldehyde in 0.1 M phosphate buffer (pH 7.4). Single oocytes were embedded in 10% gelatin, infused with 2.3 M sucrose and frozen in liquid nitrogen. Sections were cut at –11°C and picked up with a 1:1 mixture of 2.3 M sucrose and 2.0 M methyl cellulose. Sections were labeled with a rabbit antibody against yolk protein (Trougakos et al., 2001), followed by 10 nm protein A gold, and observed in a JEOL-1230 electron microscope at 60-80 kV. Images were recorded with a Morada digital camera using iTEM (SIS) software.

Quantification of EM data

ESCRT mutant germlines prepared as above were labeled with Rat anti-yolk antibody and the number of isolated MVBs and of ILV-containing yolk granules (ILVYGs) in the oocyte were counted. Vesicles containing only ILVs without significant yolk accumulation were scored as MVBs, whereas MVBs containing visible yolk accumulations were scored as ILVYGs. Oocytes were scanned in a systematic random fashion and the areas quantified were as follows: WT, 1360 μm^2; *hrs*, 2500 μm^2; *tsg101*, 1583 μm^2; *vps32*, 1060 μm^2; *vps22*, 1940 μm^2; *vps20*, 1360 μm^2. Values are the mean results from two to three different oocytes ± s.d.

We thank Helmut Krämer (UT Southwestern Medical Center, Dallas, TX), Daniel St Johnston (The Gurdon Institute and the Department of Genetics, University of Cambridge, UK), Ken Moberg (Department of Cell Biology, Emory University School of Medicine, Atlanta, GA), Erika Bach (Pharmacology Department, New York University School of Medicine, New York, NY) and Iswar Hariharan (University of California, Berkeley, CA) for reagents. We also thank Geena Wu, Sarah Daniels, Joe Hill and Joshua Schoenfeld for technical assistance and other members of the Bilder lab for helpful discussions. This work was supported by the American Heart Association award 0625181Y to T.V., by The Norwegian Research Council and FUGE, Norway to T.E.R., H.S. and A.B., by The Norwegian Cancer Society and the Novo Nordisk Foundation to H.S. and by National Institutes of Health grant R01GM068675, American Cancer Society grant RSG-07-040-01 and Burroughs Wellcome Fund Award to D.B. Deposited in PMC for release after 12 months.

References

Babst, M., Odorizzi, G., Estepa, E. and Emr, S. (2000). Mammalian tumor susceptibility gene 101 (TSG101) and the yeast homologue, Vps23p, both function in late endosomal trafficking. *Traffic* **1**, 248-258.

Babst, M., Katzmann, D., Estepa-Sabal, E., Meerloo, T. and Emr, S. (2002). Escrt-III: an endosome-associated heterooligomeric protein complex required for mvb sorting. *Dev. Cell* **3**, 271-282.

Bache, K. G., Raiborg, C., Mehlum, A. and Stenmark, H. (2003). STAM and Hrs are subunits of a multivalent ubiquitin-binding complex on early endosomes. *J. Biol. Chem.* **278**, 12513-12521.

Bache, K. G., Stuffers, S., Malerød, L., Slagsvold, T., Raiborg, C., Lechardeur, D., Wälchli, S., Lukacs, G. L., Brech, A. and Stenmark, H. (2006). The ESCRT-III subunit hVps24 is required for degradation but not silencing of the epidermal growth factor receptor. *Mol. Biol. Cell* **17**, 2513-2523.

Baker, N. E. and Rubin, G. M. (1989). Effect on eye development of dominant mutations in Drosophila homologue of the EGF receptor. *Nature* **340**, 150-153.

Bilodeau, P., Urbanowski, J., Winistorfer, S. and Piper, R. (2002). The Vps27p-Hse1p complex binds ubiquitin and mediates endosomal protein sorting. *Nat. Cell Biol.* **4**, 534-539.

Bogard, N., Lan, L., Xu, J. and Cohen, R. S. (2007). Rab11 maintains connections between germline stem cells and niche cells in the Drosophila ovary. *Development* **134**, 3413-3418.

Carlton, J., Agromayor, M. and Martin-Serrano, J. (2008). Differential requirements for Alix and ESCRT-III in cytokinesis and HIV-1 release. *Proc. Natl. Acad. Sci. USA* **105**, 10541-10546.

Chou, T., Noll, E. and Perrimon, N. (1993). Autosomal P[ovoD1] dominant female-sterile insertions in Drosophila and their use in generating germ-line chimeras. *Development* **119**, 1359-1369.

Coutelis, J. B. and Ephrussi, A. (2007). Rab6 mediates membrane organization and determinant localization during Drosophila oogenesis. *Development* **134**, 1419-1430.

Doyotte, A., Russell, M. R. G., Hopkins, C. R. and Woodman, P. G. (2005). Depletion of TSG101 forms a mammalian "Class E" compartment: a multicisternal early endosome with multiple sorting defects. *J. Cell Sci.* **118**, 3003-3017.

Hanson, P. I., Roth, R., Lin, Y. and Heuser, J. E. (2008). Plasma membrane deformation by circular arrays of ESCRT-III protein filaments. *J. Cell Biol.* **180**, 389-402.

Herz, H., Chen, Z., Scherr, H., Lackey, M., Bolduc, C. and Bergmann, A. (2006). vps25 mosaics display non-autonomous cell survival and overgrowth, and autonomous apoptosis. *Development* **133**, 1871-1880.

Hong, Y., Ackerman, L., Jan, L. and Jan, Y. (2003). Distinct roles of Bazooka and Stardust in the specification of Drosophila photoreceptor membrane architecture. *Proc. Natl. Acad. Sci. USA* **100**, 12712-12717.

Hurley, J. H. and Emr, S. D. (2006). The ESCRT complexes: structure and mechanism of a membrane-trafficking network. *Annu. Rev. Biophys. Biomol. Struct.* **35**, 277-298.

Irion, U. and St Johnston, D. (2007). bicoid RNA localization requires specific binding of an endosomal sorting complex. *Nature* **445**, 554-558.

Jekely, G. and Rorth, P. (2003). Hrs mediates downregulation of multiple signalling receptors in Drosophila. *EMBO Rep.* **4**, 1163-1168.

Kanazawa, C., Morita, E., Yamada, M., Ishii, N., Miura, S., Asao, H., Yoshimori, T. and Sugamura, K. (2003). Effects of deficiencies of STAMs and Hrs, mammalian class E Vps proteins, on receptor downregulation. *Biochem. Biophys. Res. Comm.* **309**, 848-856.

Komada, M. and Kitamura, N. (2005). The Hrs/STAM complex in the downregulation of receptor tyrosine kinases. *J. Biochem.* **137**, 1-8.

Leung, K., Dacks, J. and Field, M. (2008). Evolution of the multivesicular body ESCRT machinery; retention across the eukaryotic lineage. *Traffic* **9**, 1698-1716.

Lloyd, T., Atkinson, R., Wu, M., Zhou, Y., Pennetta, G. and Bellen, H. (2002). Hrs regulates endosome membrane invagination and tyrosine kinase receptor signaling in Drosophila. *Cell* **108**, 261-269.

Lu, H. and Bilder, D. (2005). Endocytic control of epithelial polarity and proliferation in Drosophila. *Nat. Cell Biol.* **7**, 1132-1139.

Martin-Serrano, J., Zang, T. and Bieniasz, P. D. (2003). Role of ESCRT-I in retroviral budding. *J. Virol.* **77**, 4794-4804.

Menut, L., Vaccari, T., Dionne, H., Hill, J., Wu, G. and Bilder, D. (2007). A mosaic genetic screen for Drosophila neoplastic tumor suppressor genes based on defective pupation. *Genetics* **177**, 1667-1677.

Moberg, K., Schelble, S., Burdick, S. and Hariharan, I. (2005). Mutations in erupted, the Drosophila ortholog of mammalian tumor susceptibility gene 101, elicit non-cell-autonomous overgrowth. *Dev. Cell* **9**, 699-710.

Morita, E., Sandrin, V., Chung, H. Y., Morham, S. G., Gygi, S. P., Rodesch, C. K. and Sundquist, W. I. (2007). Human ESCRT and ALIX proteins interact with proteins of the midbody and function in cytokinesis. *EMBO J.* **26**, 4215-4227.

Murthy, M. and Schwarz, T. L. (2004). The exocyst component Sec5 is required for membrane traffic and polarity in the Drosophila ovary. *Development* **131**, 377-388.

Newsome, T., Asling, B. and Dickson, B. J. (2000). Analysis of Drosophila photoreceptor axon guidance in eye-specific mosaics. *Development* **127**, 851-860.

Raymond, C., Howald-Stevenson, I., Vater, C. and Stevens, T. (1992). Morphological classification of the yeast vacuolar protein sorting mutants: evidence for a prevacuolar compartment in class E vps mutants. *Mol. Biol. Cell* **3**, 1389-1402.

Razi, M. and Futter, C. E. (2006). Distinct roles for Tsg101 and Hrs in multivesicular body formation and inward vesiculation. *Mol. Biol. Cell* **17**, 3469-3483.

Rieder, S. E., Banta, L. M., Köhrer, K., McCaffery, J. M. and Emr, S. D. (1996). Multilamellar endosome-like compartment accumulates in the yeast vps28 vacuolar protein sorting mutant. *Mol. Biol. Cell* **7**, 985-999.

Saksena, S., Sun, J., Chu, T. and Emr, S. D. (2007). ESCRTing proteins in the endocytic pathway. *Trends Biochem. Sci.* **32**, 561-573.

Schonbaum, C. P., Perrino, J. J. and Mahowald, A. P. (2000). Regulation of the vitellogenin receptor during Drosophila melanogaster oogenesis. *Mol. Biol. Cell* **11**, 511-521.

Sevrioukov, E. A., Moghrabi, N., Kuhn, M. and Krämer, H. (2005). A mutation in dVps28 reveals a link between a subunit of the endosomal sorting complex required for transport-I complex and the actin cytoskeleton in Drosophila. *Mol. Biol. Cell* **16**, 2301-2312.

Sun, W., Yan, Q., Vida, T. A. and Bean, A. J. (2003). Hrs regulates early endosome fusion by inhibiting formation of an endosomal SNARE complex. *J. Cell Biol.* **162**, 125-137.

Tapon, N., Ito, N., Dickson, B. J., Treisman, J. and Hariharan, I. (2001). The Drosophila tuberous sclerosis complex gene homologs restrict cell growth and cell proliferation. *Cell* **105**, 345-355.

Teis, D., Saksena, S. and Emr, S. (2008). Ordered assembly of the ESCRT-III complex on endosomes is required to sequester cargo during MVB formation. *Dev. Cell* **15**, 578-589.

Thompson, B., Mathieu, J., Sung, H., Loeser, E., Rorth, P. and Cohen, S. (2005). Tumor suppressor properties of the ESCRT-II complex component Vps25 in Drosophila. *Dev. Cell* **9**, 711-720.

Trougakos, I., Papassideri, I. S., Waring, G. L. and Margaritis, L. H. (2001). Differential sorting of constitutively co-secreted proteins in the ovarian follicle cells of. *Eur J. Cell Biol.* **80**, 271-284.

Tseng, A. S., Tapon, N., Kanda, H., Cigizoglu, S., Edelmann, L., Pellock, B., White, K. and Hariharan, I. K. (2007). Capicua regulates cell proliferation downstream of the receptor tyrosine kinase/ras signaling pathway. *Curr. Biol.* **17**, 728-733.

Vaccari, T. and Bilder, D. (2005). The Drosophila tumor suppressor vps25 prevents nonautonomous overproliferation by regulating notch trafficking. *Dev. Cell* **9**, 687-698.

Vaccari, T., Lu, H., Kanwar, R., Fortini, M. E. and Bilder, D. (2008). Endosomal entry regulates Notch receptor activation in Drosophila melanogaster. *J. Cell Biol.* **180**, 755-762.

Vida, T. A., Huyer, G. and Emr, S. D. (1993). Yeast vacuolar proenzymes are sorted in the late Golgi complex and transported to the vacuole via a prevacuolar endosome-like compartment. *J. Cell Biol.* **121**, 1245-1256.

Williams, R. L. and Urbé, S. (2007). The emerging shape of the ESCRT machinery. *Nat. Rev. Mol. Cell Biol.* **8**, 355-368.

Supplemental Figure S1 -

Fig. S1. Categorized phenotypic view of 2R MENE mutants. (A-L) Eye imaginal discs stained with phalloidin to detect cortical actin. Compared with WT (A), discs entirely mutant for complementation groups *MENE (2R)-A-F* (C-H) show disorganized tissue architecture, increased proliferation, actin upregulation, and no photoreceptor differentiation, all hallmarks of neoplastic TSG mutations. For description of the phenotype of other MENE mutants (B,K-L), see Table 2. Scale bar: 100 µm.

Supplemental Figure S2 -

Fig. S2. *vps28* is as an endocytic neoplastic TSG that does not control Staufen localization. (A-B) Rescue of epithelial architecture and ubiquitin accumulation in $vps28^{D2}$ mutants by Vps28 expression. Mutant cells are marked by presence of GFP are stained with anti-ubiquitin; the neoplastic TSG phenotype and the ubiquitin accumulation of $vps28^{D2}$ mutants (A) is rescued by ectopic expression of Vps28 in mutant cell (B). Single ubiquitin channel is shown in A'-B'. (C-F) Vps28 is not required for anterior localization of Staufen at mid-oogenesis. Stage 10 egg chambers containing ESCRT-I and ESCRT-II mutant germline cells and expressing GFP-Staufen are stained with phalloidin to reveal egg chamber morphology. Similarly to control egg chamber (C), both $vps28^{l(2)k16503}$ (D) and $vps28^{D2}$ (E) mutant oocytes show tight anterior GFP-Staufen localization (E; arrowhead). By contrast, *vps25* egg chambers display diffusion of GFP-Staufen towards the oocyte center (F). Scale bars: 10 µm (A-B), 50 µm (C-F).

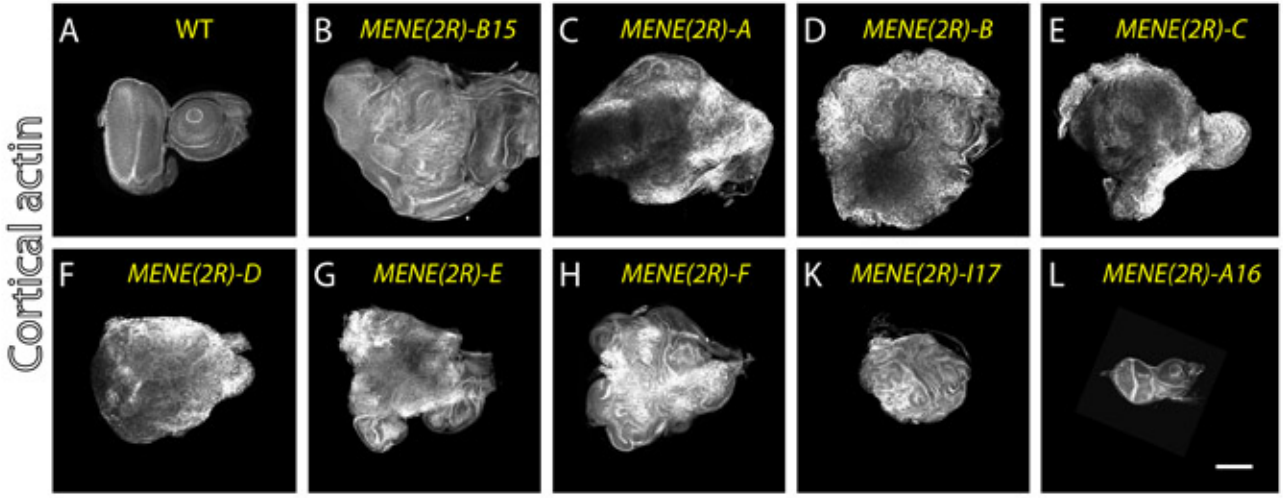
Cortical actin
A
WT
B
MENE(2R)-B15
C
MENE(2R)-A
D
MENE(2R)-B
E
MENE(2R)-C
F
MENE(2R)-D
G
MENE(2R)-E
H
MENE(2R)-F
K
MENE(2R)-I17
L
MENE(2R)-A16

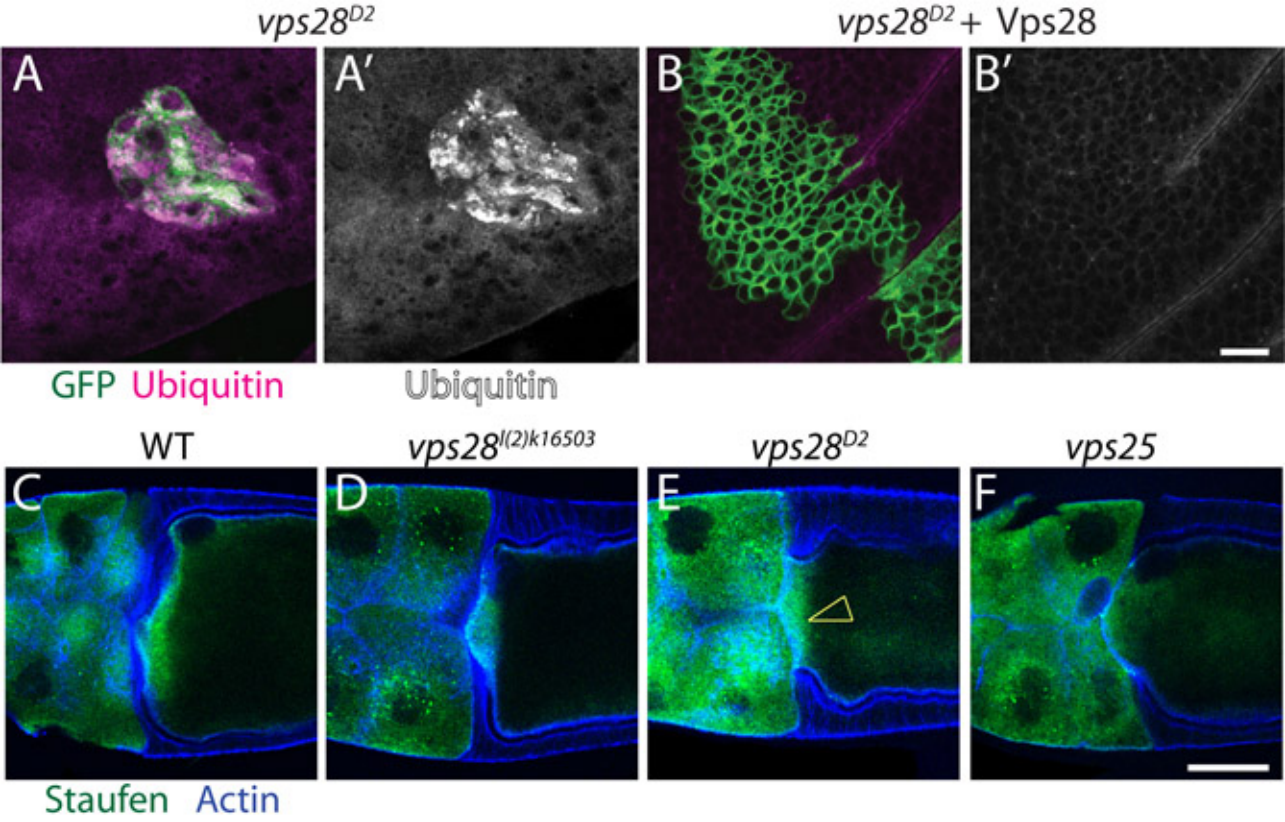
vps28D2
vps28D2 + Vps28
A
A′
B
B′
GFP Ubiquitin
Ubiquitin
WT
vps28l(2)k16503
vps28D2
vps25
C
D
E
F
Staufen Actin